IFHTSE 2016

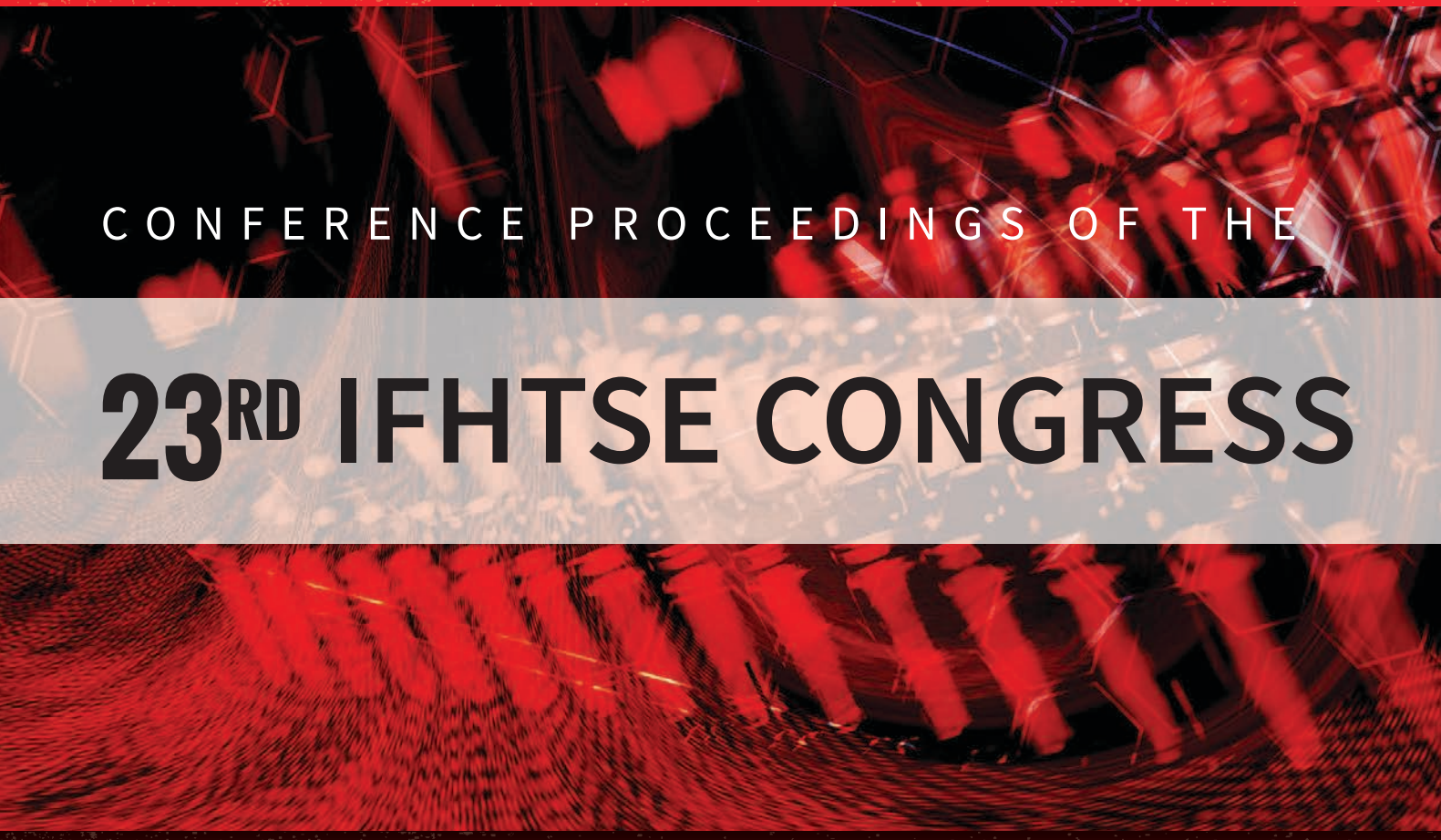

CONFERENCE PROCEEDINGS OF THE

23RD IFHTSE CONGRESS

APRIL 18-21, 2016

HYATT REGENCY

SAVANNAH, GEORGIA, USA

Organized by:

IFHTSE
INTERNATIONAL FEDERATION FOR HEAT TREATMENT AND SURFACE ENGINEERING

HTS
Heat Treating Society
ASM INTERNATIONAL

ASM
INTERNATIONAL

International Federation of Heat Treatment and Surface Engineering 2016
Proceedings of the 23rd IFHTSE Congress
April 18–21, 2016, Savannah, Georgia, USA

Metallurgical Aspects of Distortion and Residual Stresses in Heat Treated Parts

D. Scott MacKenzie, PhD, FASM
Houghton International, Inc., Valley Forge PA 19426
smackenzie@houghtonintl.com

Abstract

While modeling of quenchant behavior and microstructural response has matured, the sensitivity to variation of common metallurgical and production practices are often not considered. As an example, the variation in hardenability of the purchased material is generally not considered when predicting microstructure and residual stress. Machining practices, including worn tools and use of tooling beyond the expected life can have dramatic influence on distortion and residual stress. The quench oil chosen, and the quench part are all important variables to consider. Finally the presence of adjacent parts and the racking method can also effect the residual stress state and distortion. The effects of common metallurgical variables on the residual stress and distortion of heat treated parts are reviewed. Factors such as hardenability, segregation, and rack and fixture design are discussed.

Introduction

The problem of distortion is universal across industry. A study by Thoben (1) indicated that the 1995 losses from heat treatment alone in the German machine, automotive and transmission industry exceeded 850M € (1 Billion USD). This does not include the rest of Europe, Asia or the Americas. The problem is truly immense.

Distortion is not limited to heat treatment, but each step in the manufacturing process contributes to distortion 0. The sources of distortion follow the manufacturing process chain. Looking at distortion, the primary sources are volume changes from phase transformations and precipitation, or from deformation from either plastic or elastic deformation (Figure 1).

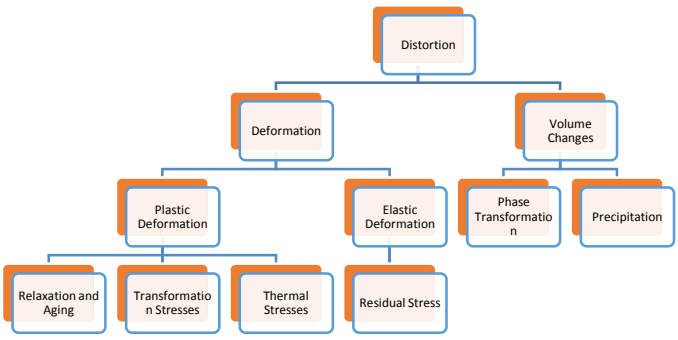

Figure 1. Global sources of distortion (2).

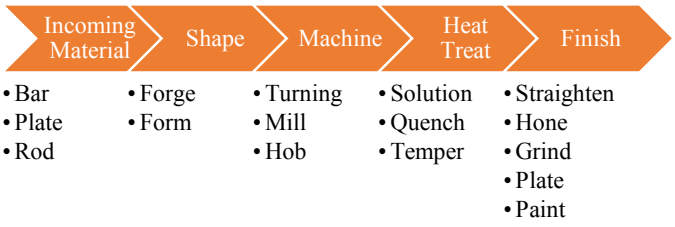

Figure 2. Typical fabrication sequence or process chain of a generic steel or aluminum component.

The literature is filled with papers trying to understand and model the distortion of components. Modeling has been used to understand the heat treatment process and the entire process chain. However, modeling is usually used to model the component under perfect conditions – new tooling, homogeneous steel, uniform heat treating conditions and quenchant. Rarely are sensitivity studies performed to look at the expected variation of distortion due to manufacturing variation.

It is the intent of this paper to review some of the possible variation due to metallurgical and manufacturing processes.

Literature Review

In the typical manufacturing process to manufacture a steel or aluminum part, incoming material is purchased; shaped by forming, forging or casting; machined; heat treated; and finish processed (final machining, plating or painting). This is illustrated in Figure 2.

There are many sources of distortion that have been identified. A fishbone chart illustrating some of the common sources of distortion is shown in Figure 3. It is not the purpose of this paper to review all the possible sources and permutations of distortion, but to highlight some of the important factors.

Prior Microstructure

The incoming raw material plays a critical role in the quality of a finished part. The prior microstructure and hardenability of the alloy grade selected, as well as the cleanliness of the incoming material affect distortion and the mechanical properties (fatigue and impact properties). This is illustrated in Figure 4.

Hippenstiel (3) evaluated the effect of prior grain size on distortion and found that finer grain size contributed to reduced distortion. He also found that by reducing the amount of grain size variation, further reductions in distortion could be achieved.

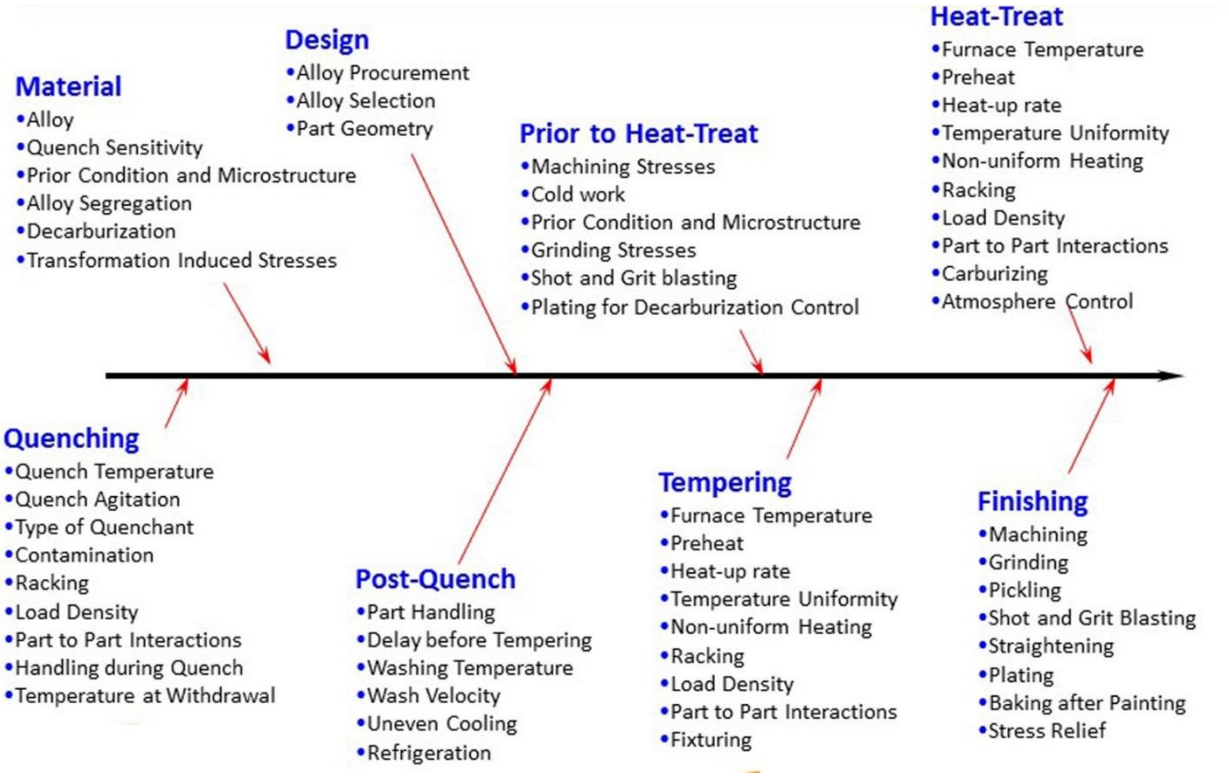

Figure 3. Fishbone diagram showing some of the many factors affecting distortion.

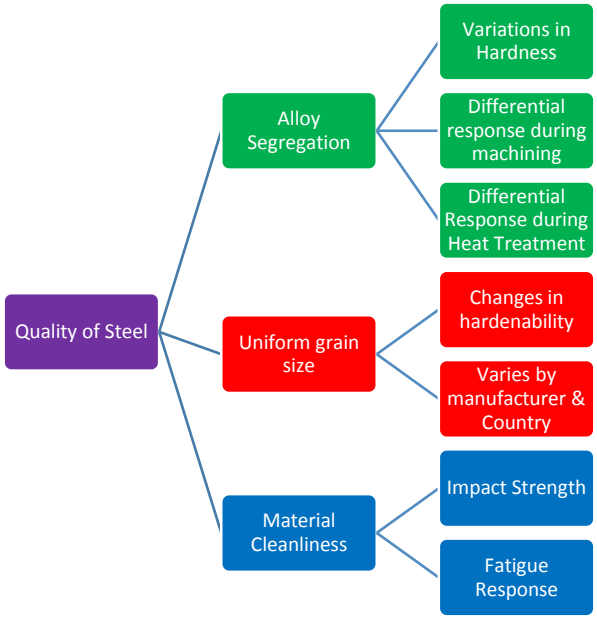

Figure 4. Quality of steel and impact on distortion and property response.

In another study (4), electro-slag remelted and vacuum melted and remelted X38CrMoV5-1 hot-work steels were examined for distortion, residual stresses, microstructure and properties. The vacuum heat treatment were varied to develop a model of phase volume fraction, residual stress and hardness. Using a Gleeble, the transformation kinetics and flow curves for the alloys were measured. A hardness after tempering was developed based on the volume fraction and hardness of each phase. An additional difficulty was the calculation after tempering was overcome by the inclusion of a coarse secondary hardening carbide. The validation of the model showed good correspondence with experiment.

The examination of the prior microstructure on the distortion of press-quenched gears was conducted by Reardon (5). In this study, 464 mm diameter AISI 8620 H steel automotive transmission gears were processed in two separate furnace loads. For the first set of gears, which were designated Series 1, the normalizing temperature that was used was 926ºC. These gears received a single normalizing cycle. This is illustrated in Figure 5.

The second set of gears, labeled Series 2, was normalized twice in succession. The first normalizing cycle they received was identical to that used for the Series 1 gears. For the second normalizing cycle, the temperature was raised to 954°C. Each group of 24 gears was subsequently processed through a gas carburizing furnace using an endothermic atmosphere at a temperature of 926ºC to generate effective case depths in the range of 0.0016 to 0.0022 m. The gears were all cooled to room temperature after carburizing was completed. They were then reheated to the austenitizing temperature of 854ºC, and individually press quenched.

The resulting out of round distortion was measured (Figure 5). It was found that the double normalized gears exhibited substantially lower distortion, and much reduced distortion scatter than the single normalized gears. The double normalized gears had a mean out of roundness of 100µm, with a standard deviation of 25.4 µm. The single normalized gears had a mean out of roundness of 330 microns, with a standard deviation of 154µm.

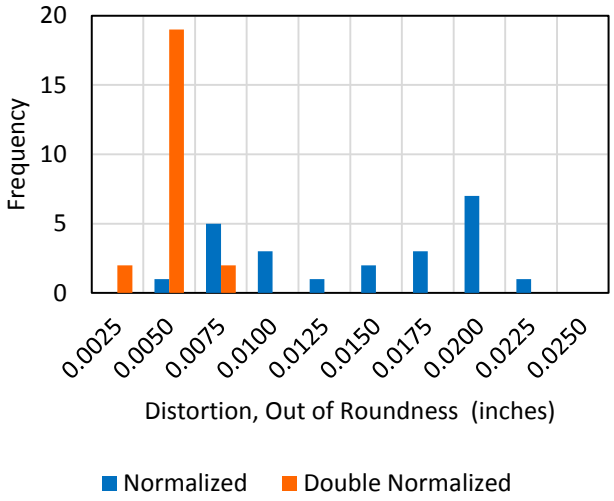

Figure 5. Effect of normalization cycle on the out of roundness of two different groups of carburized AISI 8620H gears after press quenching and normalization.

An examination of the effect of the microstructure prior to heat treatment was examined by Prinz (6). In this investigation, the microstructure of bar material was varied by normalizing, annealing or hardening and tempering. The resultant microstructures were primarily ferrite and pearlite in the normalized "as-delivered" condition, with some bainite and martensite due to the high hardenability. The annealed structure was ferrite and pearlite, while the hardened and tempered structure was tempered martensite. The extent of the distortion was evaluated by measurements before and after heat treatment of machined shafts. The effect of hardenability on the distortion of the heat treated shafts were also examined.

The results of the study showed a strong influence of the prior microstructure on the resulting distortion (Figure 6). Increasing hardenability reduced distortion. However the authors noted that it is likely that the reduced grain size from the prior heat treatments likely changed the hardenability, so the effects are compounded with prior heat treatment effects.

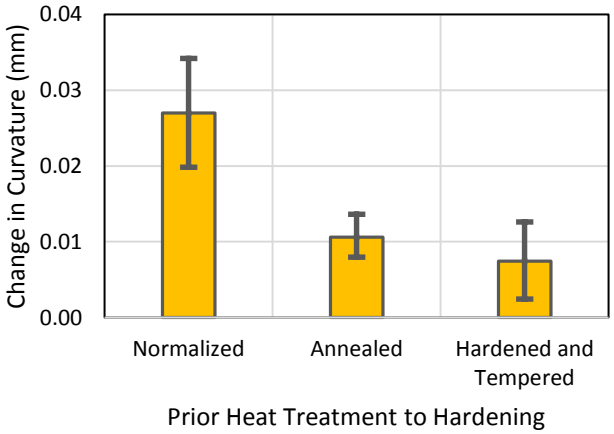

Figure 6. Variation of distortion with microstructure prior to heat treating (6).

Banding or segregation can produce a wide variation in the local hardness, even within the carburized layer (Table 1). This segregation can cause non-uniform response to heat treatment and result in uncontrolled distortion (Figure 7 & Figure 8).

These studies are all consistent, in that it shows that the prior thermal processing prior to machining and heat treatment, play a critical role in controlling the distortion of a heat treated component.

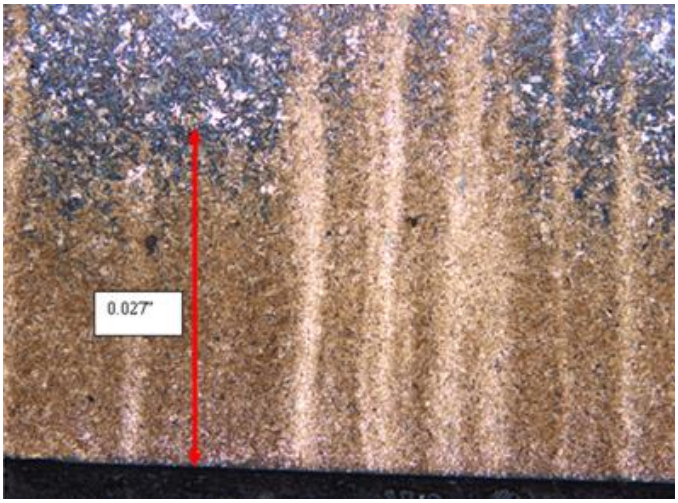

Figure 7. Segregation and banding in AISIS 4320 carburized gear showing non-uniform effective case depth (Courtesy of L. Ferguson DANTE Solutions).

Hardenability

The hardenability of a steel is influenced by its chemical composition and grainsize. The chemistry further affects the martensite start and finish temperatures, M_s. Because of variations in chemistry within an alloy specification. Even within a specific heat lot of material, the chemistry and hardenability can vary. Since higher hardenability steels are more deeply hardened than a lower hardenability steel within the same grade, it can be expected that the higher hardenability chemistry will have a higher core hardness and effective case depth. This would also indicate that the distortion would increase as hardenability increases.

Funatani (7) showed that the distortion of SCr.420 steel (a Cr case hardening grade) increased with a small variation in the Jominy End Quench hardenability. The change in over ball diameter changed from 20 µm to 80 µm as the hardness at 12.5 mm from the quenched end on the Jominy End Quench Test changed from 24 to 30 HRC (Figure 9). Hypoid ring gears of SCM430H showed that the maximum pitch angle increased as a function of the hardenability of the steel increased (Figure 10).

In one study (8), a customer was looking to increase performance of an automotive pinion gear by changing alloy from AISI 8620 to AISI 4320. the distortion of an AISI 8620 and 4320 automotive pinion gear was compared, using identical heat treating conditions. The core requirements were the same (35-40 HRC).

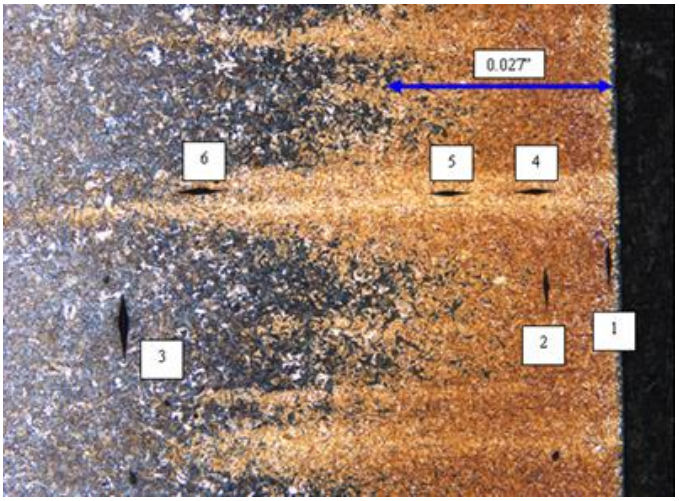

Figure 8. Segregation and banding in 4320 carburized gear showing hardness variation within case (Courtesy L. Ferguson, DANTE Solutions, Inc.). See Table 1 for hardness at locations 1-6.

Table 1. Hardness variation noted within case of carburized AISI 4320 gear (Courtesy L. Ferguson, DANTE Solutions, Inc.).

Location	Hardness (HRC)
1	56.3
2	60.3
3	33.3
4	66.3
5	60.9
6	54.9

The results of the modeling, show that the distortion of the AISI 4320 carburized pinion gear is approximately 0.15 mm – approximately one order of magnitude greater than the bow of the carburized AISI 8620 gear. This behavior was explained by the differences in the Continuous Cooling Curves of the two materials. The AISI 8620 material, with a short martensite shelf, has a significantly lower hardenability than AISI 4320. Fast cooling rates are required to achieve a fully martensitic structure. AISI 8620 also has a significant bainite bay at the expected cooling rates expected during quenching. AISI 4320 has a much higher hardenability, with a large martensite shelf. Slower cooling rates can still achieve a fully martensitic structure.

The cooling rates on opposite sides of the pinion were determined to be approximately 800°C/min and 400°C/min respectively.

For AISI 8620, the CCT diagram predicts that the microstructure would be predominately bainite with small portions of martensite and pearlite for both cooling rates. For AISI 4320, the CCT diagram predicts approximately equal portions of martensite and bainite. However, for the faster cooling rate, martensite would form earlier than for the slower cooling rate.

For 8620, during quenching, the core transforms almost completely to bainite. While some asymmetry of transformation occurs, equal amounts of bainite are formed. There is less volume expansion due to bainitic transformation, resulting in less distortion.

For AISI 4320, the core of the pinion shaft transforms to approximately equal portions of martensite and bainite. However, because of the differential cooling rates, one side of the pinion shaft transforms to martensite much earlier than the opposite side. This asymmetry of martensite formation and the accompanying volume change results in an initial bow of the pinion. Once the opposite side of the pinion transforms to martensite, a stress reversal occurs, with the final bow of 0.15 mm.

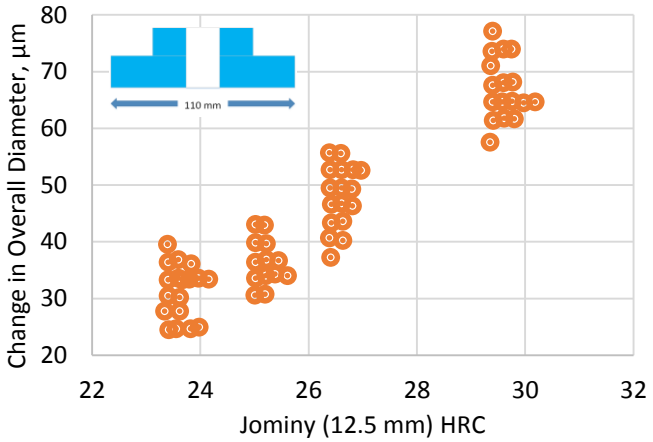

Figure 9. Influence of steel hardenability on the over ball diameter of Carburized Module 2.8 Spur gears. Gears were carburized at 920°C and quenched in 90°C oil (7).

Recommendations included increasing the agitation or modifying the racking to achieve uniform heat transfer around the circumference of the shaft.

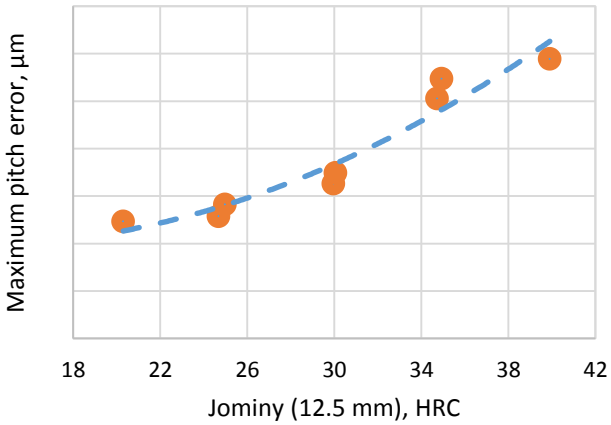

Figure 10. Influence of steel hardenability on the maximum pitch angle of hypoid ring gears (SCM420H) (7).

An investigation into the effect of variation of hardenability within heats of 16NiCrS4 carburizing steel was conducted by Stormvinter, *et al* (9). Three different heats of material (Table 2) were obtained as tubes of 71 mm diameter and a wall

thickness of 17 mm. The tubes were sectioned and machined into rings of 70 mm diameter, with a wall thickness of 16 mm and a height of 19 mm. The calculated ideal diameter, DI in mm, for Heats A, B and C were 80.47 mm, 91.73 mm and 100.82 mm. All heats satisfied the requirements for 16NiCrS4.

Table 2. Heat examined by Stormvinter et al (9).

Steel heat	C	Si	Mn	P	S	Cr	Ni	Mo	Cu
Heat A	0.2	0.07	1.00	0.12	0.41	1.01	1.03	0.13	0.17
Heat B	0.2	0.07	1.03	0.16	0.41	1.04	1.05	0.17	0.17
Heat C	0.2	0.07	1.02	0.08	0.41	1.03	1.39	0.16	0.18

The rings were first machined then stress relieved at 600°C for 5 hours. Rings were austenitized at 850°C for 1 hour with no carburizing. The rings were then quenched in an accelerated quench oil at 50°C. The rings were measured for distortion before and after heat treatment. The results of the measurements at the inner and outer diameters are shown in Figure 11 and Figure 12. The hardness of the rings were identical within the error of the hardness measurement.

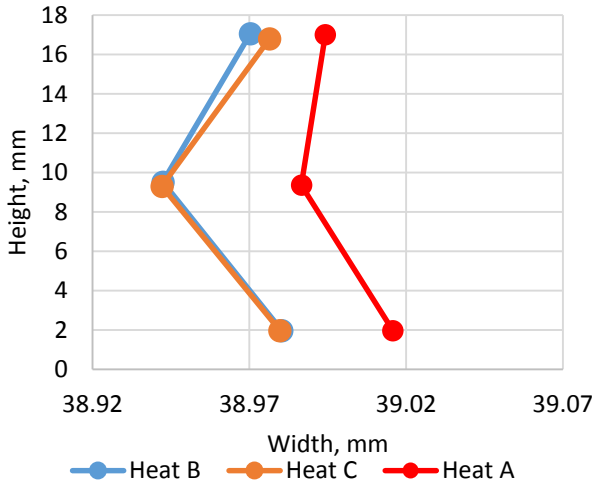

Figure 11. Radial distortion of the inner surface of the heat treated rings. The inner surface becomes convex. The inner diameter shrinks for steel heats B and C, but grows for A. The nominal inner diameter is 38.98 mm.

For ring components, a lower hardenability alloy would tend to cause the ring to become thinner and have a larger overall diameter. For higher hardenability alloys, the ring would become thicker and tend to shrink.

The effect of distortion was also studied (9) on production vehicle crown wheels. In this study the crown wheels were manufactured from forgings of 17NiCrMoS6-4 using a steel from a single steel mill. All crown wheels were machined and heat treated at the same time to minimize unknown influences. The distortion of the crown wheels was then measured using a coordinate measuring machine (Figure 13).

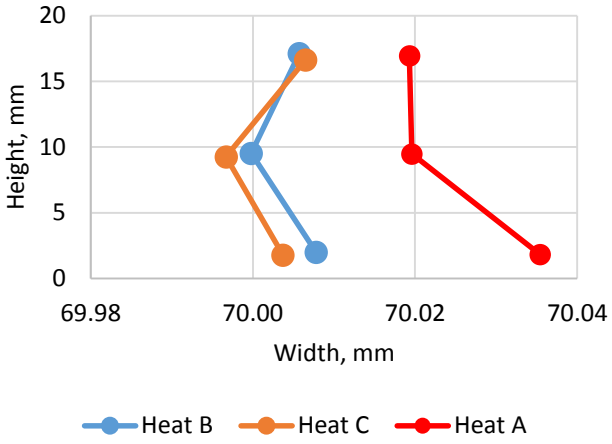

Figure 12. Radial distortion of the outer surface of the heat treated rings. The nominal outer diameter is 70.01 mm. The surfaces become concave.

Four mill heats of steel were examined, and the results show that there is a correlation between the measured hardenability of the steel, and the resultant distortion of the wheel. Different heats, with different hardenability, affected the distortion of the crown wheel.

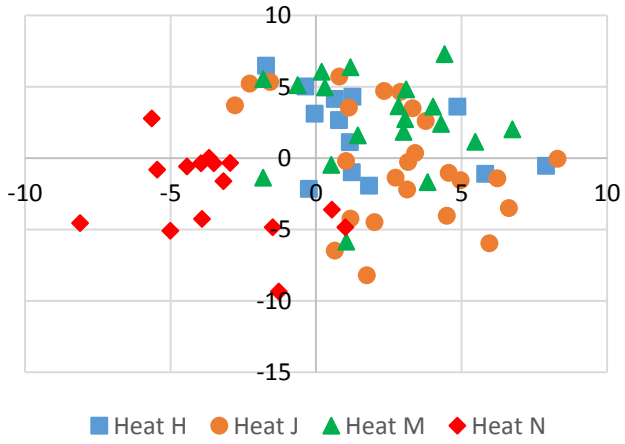

Figure 13. Score scatter plot from principal component analysis. The first PCA component and the Second PCA component are represented by the x-axis and y-axis respectively. Each dot represents the relative distortion of a crown wheel. The distortions are examined corresponding to different steel heats.

Machining

Prior operations such as machining create residual stresses at the surface. This stress is relieved during heat treatment, resulting in distortion.

During turning or milling operations, the work piece is held fixed by a chuck or jaws. The method of holding the work piece can result in residual stresses. In one study (10), 100Cr6 (SAE 52100) bearing rings were evaluated on the influence of cutting speed, depth of cut, and feed rate on the roundness. Two different types of clamping mechanisms were used: a mandrel clamp and segmented jaws.

The study showed (Figure 14) that the residual stresses in the tangential direction of the two rings had a mean residual stress for the different clamping methods were nearly identical with a mean residual stress of 600 MPa. The segmented jaws show a periodicity of three around the circumference, with the tangential residual stress varying between 500 and 700 MPa. The mandrel chuck showed a slight periodicity of 6, but varied to a much less greater degree, with the variation between approximately 590 and 620 MPa.

The segmented jaws had a segment of approximately 120°, however, the real contact was limited to a single point in the middle of each segment. Therefore the clamping forces are induced at three locations 120° apart. This results in the ring bulging at these locations. The mandrel supports the bearing uniformly around the circumference, resulting in a uniform residual stress.

Further work was conducted by Grote (11), comparing the residual stresses generated by different methods of clamping a work piece during internal turning.

The influence of cutting parameters on residual stresses were also investigated for rings that were clamped by a mandrel. Four cutting parameters were examined: cutting speed, nose radius, depth of cut and feed rate. The influence of the different parameters is shown in Figure 15. The parameters used for the DOE is shown in Table 3.

Heat Treatment

Heat treating and quenching is a complex business. The configuration of parts is endless, as is the types of furnaces available for heat-treating. Numerous variables in the quenching process alone govern the ability of a part to meet distortion requirements (Figure 3). Heat-treating is a constant balancing process. It is important to balance the ability of the material to achieve properties, while at the same time control distortion.

Multiple heat transfer regimes occur during the quenching process at the same time. These heat transfer mechanisms change as a function of the quench path. Further changes occur as the quenchant oxidizes, complicating the analysis. Agitation and racking interact, changing heat transfer at different locations on the part. There is no quantitative method to understand the interaction of fluid flow and the part, with the accompanying changes in time dependent heat transfer.

Phase transformations result in volume changes and transformational strains. Diffusional processes (pearlite + ferrite, and bainite) and non-diffusional processes (martensite) are time and temperature dependent.

Sources of stress and strain include thermal strain, creep and strains from phase transformation further complicate the business of heat treating (Figure 16).

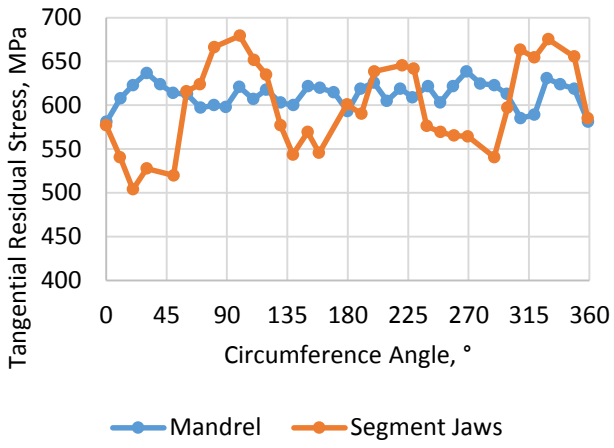

Figure 14. Residual stress distribution around a ring circumference depending on the clamping technique used.

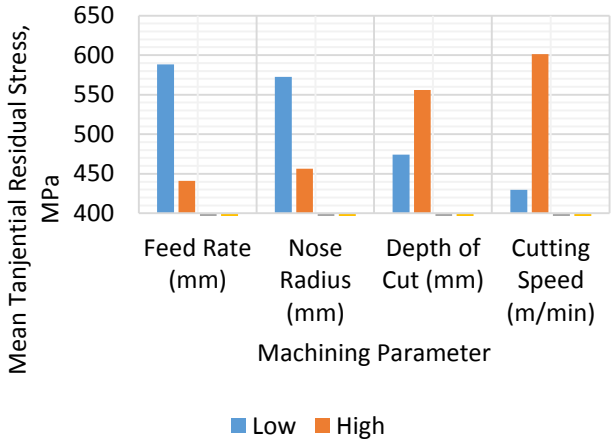

Figure 15. Results of DOE conducted by Nowag, et al, on 100Cr6, using a TiN tool and a 3% emulsion coolant.

Table 3. Levels used by Nowag et al, examining the effects of machining parameters on the external turning of 100Cr6 (SAE 52100).

	Feed Rate	Nose Radius (mm)	Depth of Cut (mm)	Cutting Speed (m/min)
Levels	0.3	0.8	0.7	200
	0.6	1.2	1.2	300

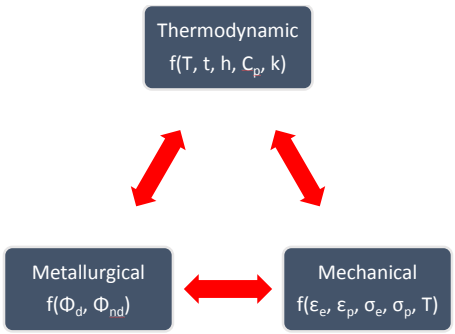

Figure 16. Interrelationships of primary variables on a heat treated part and resulting residual stress and distortion.

Thermal stresses result from thermal gradients: surface to center and surface to surface. Surface to surface thermal gradients result from differential heat transfer around the surface of the part. This could be from inadequate agitation during quenching, or from thinner sections (gear tooth) attached to a thicker or heavier body. Surface to center thermal gradients are due to the surface cooling faster than the interior, limited by the thermal diffusivity of the part. As a general rule, the faster the quench, the greater the thermal gradient.

Transformation stresses are complex in heat treating. This is a coupled stress related to phase changes that occur during heat treatment. As a part is heated, the volume expands due to thermal expansion. As the temperature increases thru the first critical temperature, the volume decreases as ferrite transforms to austenite. The volume then expands due to thermal expansion of austenite until the steady state temperature is reached.

During quenching, there is a volumetric contraction as the work piece cools. As austenite transforms, there is a volume expansion. Martensite expands the most, as a function of the carbon content. Other phases can form, such as bainite or pearlite, which have much smaller volumetric expansion. Generally outer fibers transform first, then inner fibers. This is further complicated by the effect of martensitic transformation start temperatures. Depending on the relative M_s temperatures and the thickness of a part, it is often possible that the core will transform first due to a much higher M_s temperature. As the remaining part transforms, a stress reversal occurs.

An investigation into the influence of carburizing parameter on the distortion behavior of stepped shafts was conducted by Bahnsen *et al* (12). In this study, the influence of prior microstructure, carburizing depth, surface carbon content, process sequence, carburizing temperature and the secondary hardening temperature on distortion were evaluated in a DOE. The results are shown in Figure 17 and Figure 18.

The largest dominating effect was found to be the carburizing depth. All geometrical parameters exhibited a significant sensitivity to the depth of carburizing. Other parameters showed an effect, but not necessarily statistically significant for this investigation.

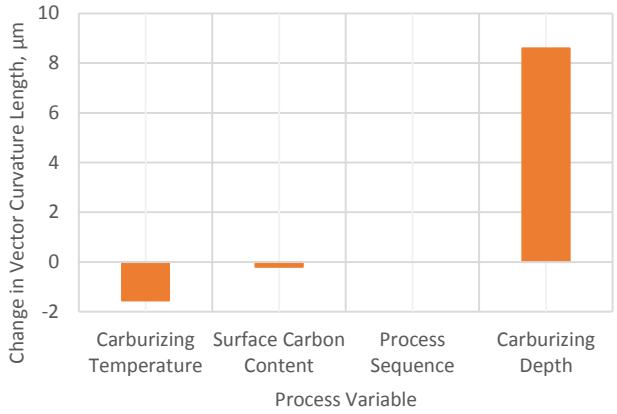

Figure 17. Effects carburizing parameters on curvature vector length of an AISI 5120 carburized shaft 14 mm in diameter.

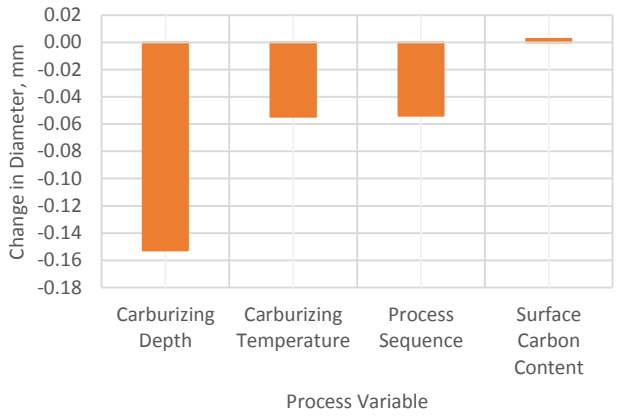

Figure 18. Effects of carburizing parameters on the change in diameter of a AISI 5120 carburized 14 mm shaft.

An investigation into the distortion behavior at elevated carburizing temperatures was conducted by Kleff *et al* (13). Heavy duty transmission components with deep case requirements require long furnaces times to satisfy case depth requirements. The use of elevated carburizing temperatures would significantly reduce the time required for carburizing, and increase production rates. Using a selection of various parts, the distortion was measured after carburizing at 930°C, 980°C and 1050°C. Alternative heating and cooling profiles were also investigated.

Two different grades of steel were used in this study: either 18CrNiMo7-6 or 20MnCrB5. Both grades were processed as a conventional heat with Al or N added. A modified grade with additional Ti (0.002%) and Nb (0.03-0.04%) for grain size control. Case hardening was performed by gas carburizing at the carburizing temperature. The parts were cooled to the hardening temperature and oil quenched. An iso-thermal step at 800°C was added to achieve more homogeneous temperature distribution in the part.

Examination of the radial run-out of the helical bevel gears, as well as the outer and inner diameters was conducted. The radial run-out was found to be small for all temperatures processed.

The inner and out diameters showed a slight increase after carburizing at 940°C and 980°C (≤ 200 µm), or stayed nearly constant when carburizing at 1050°C (Figure 19).

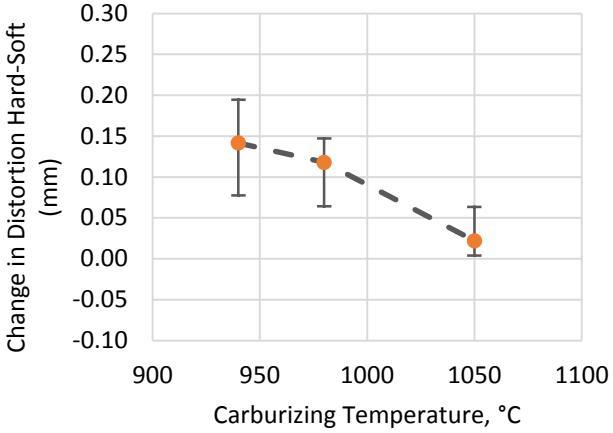

Figure 19. Results of carburizing temperature on the bore diameter of a 191.85mm diameter H6 helical bevel gear.

No negative influence on higher carburization temperatures were observed, provided that an intermediate heating step to insure homogeneous temperature distribution is included.

Since the primary focus was to investigate the use of higher temperatures to shorten production time, quenching parts directly from the carburizing temperature instead of the hardening temperature of 850°C was investigated. Helical gears were carburized at 930C, 980C and 1050C and quenched directly from the carburizing temperature. The results of bore diameter distortion quenched from the hardening temperature of 850°C is shown in Figure 20. Bore diameter distortion quenched directly from the carburizing temperature is shown in Figure 21.

The tooth sections and the bore of the gear showed significantly more scatter of distortion critical dimensions when quenched directly from the carburizing temperature. The tooth flank deviation increased significantly so that more stock would have to be removed. However, this increases the cost of grinding. The results showed that cooling down to the hardening temperature was necessary to achieve good distortion control and process capability.

Quenching

The literature of quenching and control of distortion is as immense as the problem of distortion in industry. The author will try and cover the high points.

A comparison of the distortion resulting from different quenching methods (traditional oil and high-pressure gas quenching) to the same hardness, and the racking method was conducted by Jurci (14). Helical gears and mating pinions made from low carbon structural steels were gas or low pressure carburized to an effective case of 0.7 mm. The dimensional distortion (shrinkage & growth) and the shape distortion (roundness, flatness and tooth deviations) were measured. They also measured the distortion as a function of position in the rack.

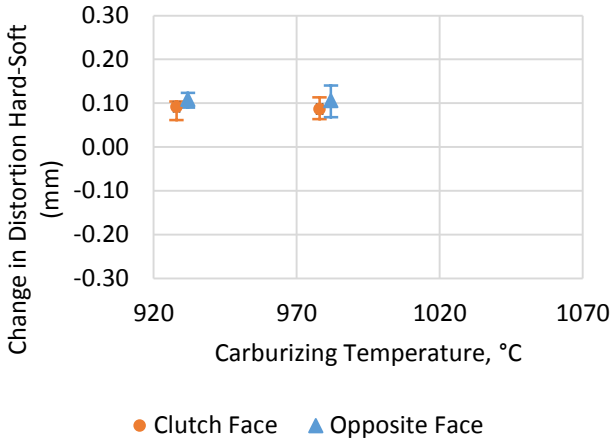

Figure 20. Influence of cooling down from the carburizing temperature to the hardening temperature of 850C on the distortion of AISI 5120 helical gears.

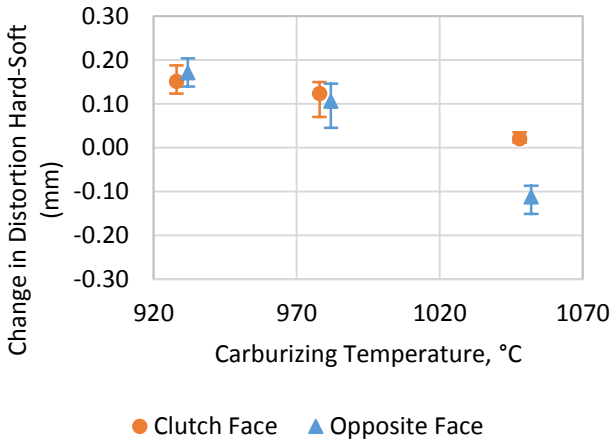

Figure 21. Influence of quenching directly from the carburizing temperature on the distortion of AISI 5120 helical gears.

The authors found significant reduction in distortion using gas-pressure quenching than the traditional oil quenching. However, they found that the use of nitrogen gas as a quenchant lead to higher out-of-flatness than oil quenching. They also observed a greater scatter in the results with gas quenching. This was attributed to inhomogeneity of gas flow with in the quenching chamber.

Braun (15) reviewed the effects of racking and condition of the oil on the resultant distortion of steel components. He found that as an oil aged, greater distortion resulted.

In another study (16), the viscosity and cooling curve was evaluated. A single viscosity base oil, and different quantities of a high viscosity (450 cSt at 40°C) were mixed. A standard speed improver quantity was added to the mixtures. Cooling curves were measured using the JIS K2242 silver probe. They showed that the speed increased from 90°C/s to 100°C as the viscosity increased to approximately 100 cSt. However, they found that the surface hardness of S45C decreased from HRC 55 to HRC 29 as the kinematic viscosity increased. They attributed the improved quenching performance at low

viscosities to the composition of the base oils having a low boiling point fraction.

A comparative study comparing the residual stresses and distortion in cylindrical components of AISI 5160H spring steel quenched at various temperatures of 25% poly-alkylene glycol (PAG) and compared to an accelerated quench oil was conducted by Sarmiento (17).

The results showed that no residual stresses were measured in cylinders quenched in either PAG or quench oil for diameters of 13.5 and 20 mm.

In a sensitivity study of quenching variables (Orientation, Slenderness ratio, M_s temperature, Quench Path and Immersion Rate), MacKenzie (18) examined the effect of the primary quenching variables on the hoop and axial stresses in simple cylinders. This study found that the orientation (horizontal or vertical) and the M_s temperature were the primary main effects for increasing radial and hoop stresses.

Racking in a vertical fashion increased the hoop stress, as did decreasing the martensite start temperature. Radial stresses were decreased by racking vertically, while decreasing the martensite start temperature increased radial stresses. The immersion rate was shown to have little effect on the residual stresses as the part cooled. The quench path, specifically the stability of the vapor phase, caused increased residual stresses. A more stable vapor phase resulted in reduced residual radial and hoop stresses. This was thought to be due to decreased thermal gradients present. This result was unexpected, and was thought to be associated with the alloy selected (41XX). This alloy has a large hardenability, so decreased initial thermal gradients would show less resultant residual stresses.

Arimoto (19) reviewed the status of quenching Fe-Ni alloys, and modeling residual stresses. His work showed that transformation plastic strain is generally similar to plastic strain during heat treatment. Plastic strain is mainly produced during rapid cooling during quenching, while transformation plastic strain is due to martensitic transformation. Both the strain distributions show a tendency of the mirror symmetry especially in circumferential and axial components.

Liscic (20) indicated that there are three simultaneous process occurring during the heat treatment process. He also proposed a new quenching technology of utilizing both a volume of gas, and dispersed liquid nitrogen, to specifically control heat extraction and heat transfer to minimize distortion and residual stresses. This method would be amenable to automated control.

Narazaki (21) predicted the heat transfer coefficients and applied them to a steel helical gear. Using the Japanese silver probe, an estimate of the heat transfer coefficient was determined by the lumped method. They found that the difference in material between the silver probe and the steel (SCr420H) gear affects the minimum temperature of the vapor blanket phase. The high conductivity of the silver rod probe resulted in stabilizing the vapor phase, with the result of lowering the minimum temperature of vapor blanket.

Funatani (7) reviewed the effects of quenchant and quenchant temperature on the distortion of SCM420 bearings 80 mm in diameter by 44 mm tall. As the heat extraction speed increased, hardness increased, but elliptical and cylindrical distortion also increased (Figure 22). As the temperature of the quenchant was increased, hardness and distortion also decreased (Figure 23).

Racking and Fixturing.

The impact of racking and fixturing on 120 mm diameter 20MnCr5 (SAE 5120) gear blanks was investigated by Clausen (22). In this study, gear blanks were carburized and quenched. During carburizing, the disks supported by 2-point loading or three point loading. Parts were preheated at 850°C and carburized at 940°C to obtain a carburized depth of 0.8 mm. Quenching was accomplished high pressure nitrogen. Measurements were carried out before and after heat treatment. It was determined that the method of racking was the most critical factor affecting gear blank distortion (Figure 24 and Figure 25).

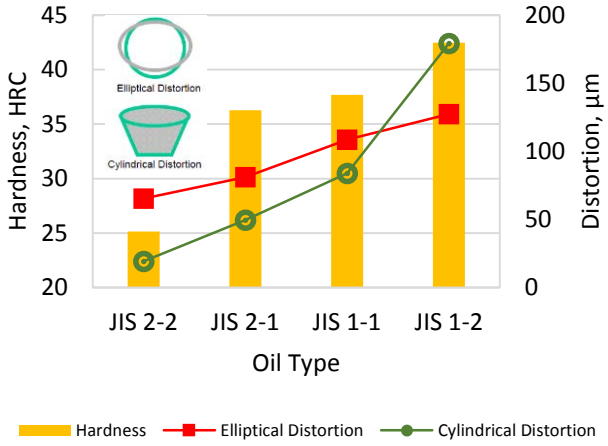

Figure 22. Comparison of quench oil selection for distortion control. SCM420 bearings (80 mm in diameter by 44 mm thick), quenched into oils of increasing speed.

Base grids used to support work are expensive, and must be replaced at routine intervals. To save money, maintenance of these grids is delayed or neglected. As these grids are used, distortion of the grid occurs. Takahashi (23) investigated the distortion of SCM420H helical gears with controlled hardenability. He found that flatness of the gears decreased as a function of time of use of the base grid (Figure 26).

In another study, MacKenzie (24) used CFD and FEA to minimize the distortion of SAE 8620 pinion gears. The gears were originally rack in a pyramid on a grid and quenched in a cold, medium speed oil. Examination of the distortion showed that the pinions would bow along the shaft up to 2 mm. An alternative method of racking and quenching in mar-tempering oil was proposed and modeled. A CFD model was created for the entire quenching system and velocity vectors established. These velocity vectors were applied as to the FEA model of each pinion gear as a boundary condition. A look-up table of heat transfer coefficient as a function of velocity and surface temperature was applied to the FEA model.

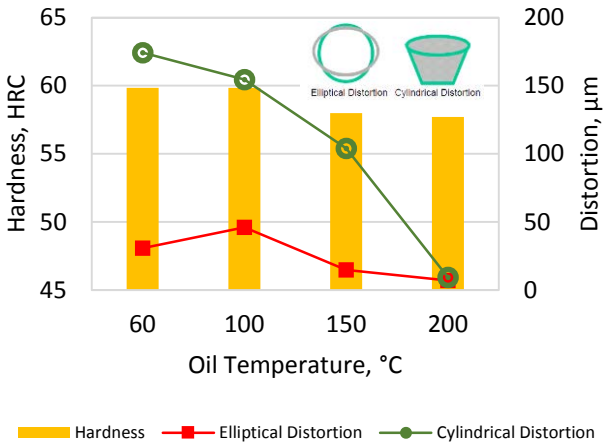

Figure 23. Comparison of quench oil temperature for distortion control. SCM420 bearings (80 mm in diameter by 44 mm thick), quenched into oils at different temperature.

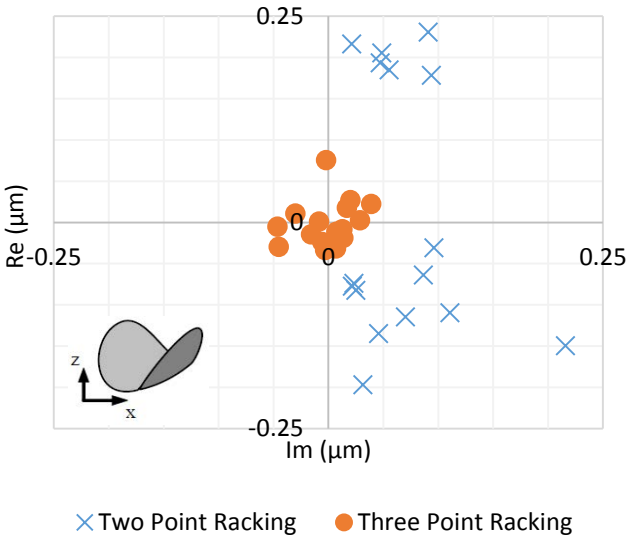

Figure 24. Change in the amplitude of the outer radius dependent on the method of loading.

The predicted bowing of the pinion was predicted to be less than 0.20 mm. Validation of the model showed that the model over-predicted the distortion, with the actual bowing of the pinion shaft averaging 0.12 mm. This reduction in distortion on this single part resulted in a documented $17,000,000 savings in rework, scrap, straightening and warranty issues.

Conclusions

The control of distortion and residual stress is a complex undertaking. Great strides have been made in the modeling and simulation of machining, heat treatment and carburizing. However the best modeling efforts can be undermined by variations in process. Dull tools, feeds and speeds and even clamping methods result in changes and variations in residual stress and distortion.

The steel making process and forming processes, with the variables of grain size, grain flow, prior microstructure and segregation can vastly effect ease of machining, as well as response to heat treatment.

While a great deal of attention has been made to control of residual stress and distortion in heat treating and quenching, these can be undermined by improper attention to the details of grid and fixture life or the changes in quenching due to oxidation of the quenchant.

It is an understanding of the entire process, and specific operations and complexities that control residual stress and distortion. These specific variables can change from machine to machine, or from vendor to vendor. Only by extreme attention to detail and attendant process variables can true distortion control be achieved.

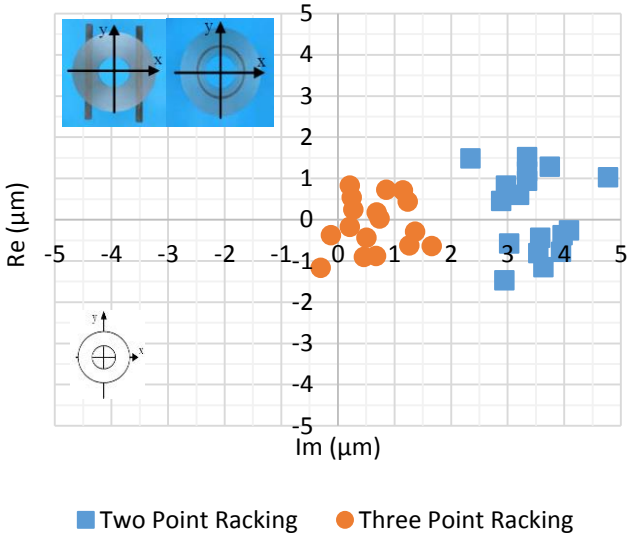

Figure 25. Change in flatness (amplitude of dish slopes) dependent on the type of racking support.

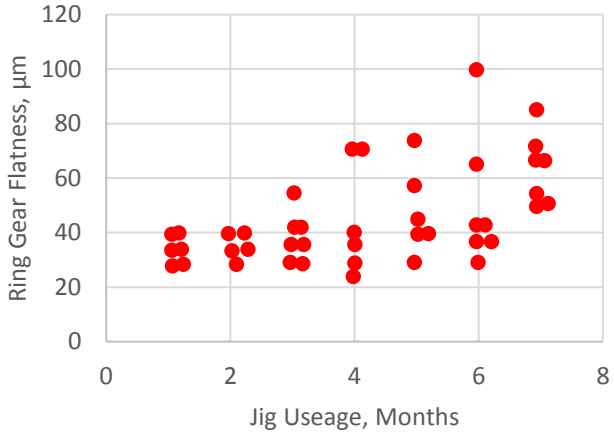

Figure 26. Effect of time-in-use of base grids on the flatness of SCM420H helical gears. Increased distortion and scatter increased as the in-use grid time increased.

Acknowledgments

I would like to thank the management of Houghton International, Inc., for allowing me to present this modest review at the 2016 ASM IFHTSE Advanced Thermal Processing World Congress.

References

1. *Distortion Engineering.* **Thoben, K.-D., et al.** 4, 2002, HTM, Vol. 57, pp. 276-282.

2. *From Single Production Step to Entire Process Chain - the Global Approach of Distortion Engineering.* **Zoch, H-W.** Bremen, Germany : s.n., 2005. IDE 2005. p. 3.

3. *Metallurgical and production-related protocols to reduce heat-treatment distortion in the manufacture of gear components.* **Hippenstiel, F.** [ed.] H-W. Zoch. Bremen, Germany : s.n., 2005. IDE 2005. pp. 57-64.

4. *Comparison of different remelted hot-work tool steels and their distortion, residual stresses and other properties. Experiments and Simulations.* **Schützenhöfer, W., et al.** Bremen, Germany : s.n., 2005. IDE 2005. pp. 65-72.

5. *Controlling Distortion in Heat Treatment Through Press Quenching.* **Reardon, A.** April 2015, Thermal Processing, pp. 24-29.

6. *Metallurgical influence on distortion of the case-hardening steel 20MnCr5.* **Prinz, C., et al.** [ed.] T. Lubben H-W. Zoch. Bremen, Germany : s.n., 2005. IDE 2005. pp. 75-82.

7. *Distortion control via optimization of cooling process and improvement of quench oils.* **Funatani, K.** Bremen, Germany : s.n., 2008. IDE 2008. pp. 265-274.

8. *Effect of Alloy on the Distortion of Oil Quenched Automotive Pinion Gears.* **MacKenzie, D. S. and Ferguson, B. L.** Shanghai, China : s.n., 2010. International Conference on Thermal Process Modeling and Computer Simulation.

9. *Effect of Hardenability and Quenching on Distortion of Steel Components.* **Stormvinter, A., et al.** Bremen, Germany : s.n., 2015. IDE 2015. pp. 39-46.

10. *Effect of Machining Parameters and Clamping Technique on the Residual Stresses and Distortion of Bearing Rings.* **Nowag, L., et al.** Bremen, Germany : s.n., 2005. IDE 2005.

11. *Distortion Engineering in Turning Processes with Standard Clamping Systems.* **Grote, C., Brinksmeier, E. and Garbrecht, M.** Bremen, Germany : s.n., 2008. IDE 2008.

12. *Influence of Carburizing on Distortion Behaviour.* **Bahnsen, C., et al.** Bremen, Germany : s.n., 2005. IDE 2005. pp. 235-242.

13. *High Temperature Carurization - Influences on Distortion Behaviour of Heavy-Duty Transmission Components.* **Kleff, J., et al.** Bremen, Germany : s.n., 2005. IDE 2005. pp. 227-234.

14. *Investigation of Distortion Behaviour of Machine Components due to Carburizing and Quenching.* **Jurci, P., et al.** Berlin, Germany : s.n., 2007. IFHTSE 5th International Quenching and Control of Distortion Conference. p. 39.

15. *Influence of the Quenching Process on the Microstructure and Distortion of Heat Treated Parts with Particular Emphasis on Quench Oils.* **Braun, R.** Bremen, Germany : s.n., 2007. IFHTSE 5th International Conference on Quenching and Control of Distortion. p. 47.

16. *The Influence of Cooling Characteristics and Viscosity on the Hardening Behaviour of Steels.* **Tomita, Y., et al.** Berlin, Germany : s.n., 2007. IFHTSE 5th International Conference on QUenching and Control of Distortion. p. 54.

17. *Modeling Residual Stresses in Spring Steel Quenching.* **Sarmiento, S., et al.** Indianapolis, IN : ASM International, 2001. Heat Treating 2001 - Including Quenching and Distortion.

18. *Effect of Quenching Variables on Distortion and Residual Stresses.* **MacKenzie, D. S. and Lambert, D.** Indianapolis, IN : ASM International, 2003. Proceedings of the 22nd Heat Treating Society Conference and the 2nd International Surface Engineering Congress.

19. *Historical Review of Resdual Stress in Quenched Fe-Ni Alloy Cylinders and Explaination of Its Origin Using Computer Simulation.* **Arimoto, K. and Funatani, K.** Detroit, MI : ASM International, 2007. Proceedings of the 24th ASM Heat Treating Society Conference.

20. *History and Perspective of Controllable Heat Extration During Quenching.* **Liscic, B.** Indianapolis, IN : ASM International, 2001. ASM 2001 Heat Treating Society Conference.

21. *Validation of Estimated Heat Transfer Coefficients during Quenching of Steel Gear.* **Narazaki, M., et al.** Berlin, Germany : s.n., 2007. IFHTSE 5th International Quenching and Control of Distortion Conference.

22. *Identification of Process Parameters affecting Distortion of Disks for Gear Manufacture - Part II: Heating, Carburizing and Quenching.* **Clausen, B., et al.** Bremen, Germany : s.n., 2008. IDE 2008. pp. 41-50.

23. ***Takahashi, A., Morishima, T. and Yamada, H.*** *6, 1990, Journal of the Japanses Heat Treating Society, Vol. 30, p. 301. 24. Control of Residual Stress and Distortion.* ***MacKenzie, D. S.*** *s.l. : ASM International, July 2007, Heat Treating Progress, p. 47.*